An Accurate Illumination Model for Objects Coated with Multilayer Films

H. Hirayama,[†] K. Kaneda,[†] H. Yamashita,[†] and Y. Monden[‡]

[†]Faculty of Engineering, Hiroshima University, Japan
[‡]Interdisciplinary Faculty of Science and Engineering, Shimane University, Japan

Abstract

This paper proposes an accurate illumination model for rendering objects coated with multilayer films. Optical phenomena of multilayer films are caused by reflection, refraction, interference, and absorption of light inside each layer of multiple films, and these physical phenomena are complicatedly related with each other. The proposed method calculates composite reflectance and transmittance of multilayer films, taking into account all the physical phenomena described above, and visualizes the optical phenomena caused by the multilayer films accurately. The illumination model proposed in the paper can handle both smooth surface and locally smooth rough surfaces. Several examples of objects coated with various kinds of films demonstrate the usefulness of the proposed method.

1. Introduction

It happens so frequently to see optical effects caused by multilayer thin films in our daily lives, and the effects are so exquisite. For examples, rainbow colors appear on the surface inside a sea shell or on a multi-coated lens of glasses, and the color changes greatly, depending on the viewing direction and wavelength of light. Such optical phenomena of multilayer films are caused by reflection, refraction, interference, and absorption of light inside each layer of multiple films, and these physical phenomena are complicatedly related with each other.

Diffraction[1] has similar optical effects to those of the thin films. Rainbow colors appear on a diffraction grating[2] and the surface of a compact disk[3]. The effects also originate from interference of light, but the path of the light ray which causes interference is quite different. In diffraction, transmitted light from a grating or reflected light from a dumpy surface interacts with each other, while in multilayer films, both reflected and refracted of light from each boundary of layers of films interact with each other. The process of interference of light inside multilayer films is more complicated.

Multilayer films are also used in industry, for example, optical lenses and filters for optical equipments, windowpanes of buildings, and so on. They are designed to have a good optical efficiency or a pleasant appearance. Traditional methods for evaluating the optical properties of films, such as graphs of reflectance and transmitance of the films, are not helpful for better understanding the properties of multilayer films, as the properties change considerably depending on both direction and wavelength of light. Therefore, it is desired to visualize optical effects of multilayer films in the design process.

2. Related work

Methods for rendering optical phenomena caused by thin films or layered objects have been developed since 1990. These illumination models for rendering films are classified into four types (see Fig. 1): Single-layer Film Primary Reflection and refraction (SFPR), Single-layer Film Multiple Reflection and refraction (SFMR), Multilayer Film Primary Reflection and refraction (MFPR), and Multilayer Film Multiple Reflection and refraction (MFMR).

The simplest illumination model is a SFPR model, which can render optical effects of a single layer film, such as soap bubbles[4] and Newton's ring[5], taking into account only primary reflection and refraction. The illumination model, however, has limitation both in objects and accuracy.

A more accurate model for a single layer film is a SFMR model. In the illumination model, multiple reflection and refraction are taken into account, and soap bubbles[6, 7], optical
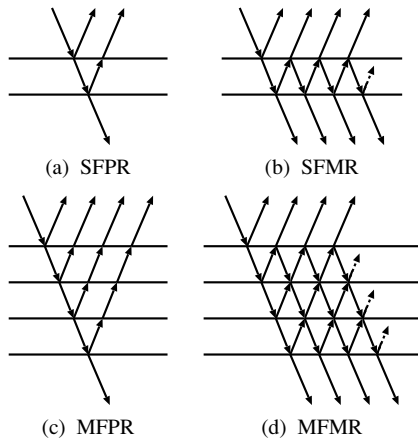
Figure 1: *Types of rendering models.*

Figure 2: *Optical phenomena due to multilayer films.*

phenomena of Newton's ring[8], optical effects of paints[9], and metric objects coated with a thin film[3] were rendered.

A MFPR model was used to render a human skin[10] realistically. The method takes into account primary reflection and refraction of light. At the same time, it considers scattering of light under the skin. Using a MFPR model, pearls[11] were also rendered. In the illumination model, interference of light inside multilayer media are also taken into account.

To accurately render objects coated with multilayer films, a MFMR model should be used. Metals coated with multilayer media[12] were rendered using a MFMR model, but the illumination model[12] cannot render the effects of interference, because the method does not consider the phase of light waves.

To address the problem and accurately render optical phenomena caused by multilayer films, we have developed a generalized MFMR illumination model[13] based on wave optics. The proposed method takes into account not only multiple reflection and refraction but also interference of light inside the multilayer films. In the illumination model, spectral distributions of light are computed, as interference of light inside multilayer films greatly depends on light wavelength. The spectral distributions are subsequently converted into RGB color components for display on a color monitor, taking into account human spectral tristimulus values.

Furthermore, we have improved the illumination model to render not only dielectric films but also semiconductive and/or metallic films[14], taking into consideration complex refractive indices, which semiconductive and metallic media have. Employing the illumination model, objects coated with various kinds of multilayer films can be rendered. However, the method can only handle ideally smooth surfaces, that reflect and/or transmit a light ray only in mirror direction and/or direction obeying Snell's law.

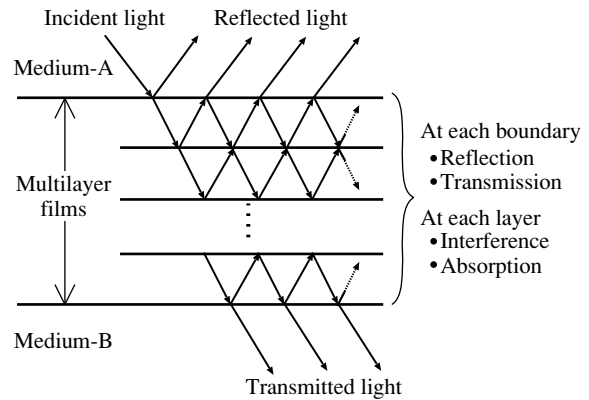In this paper, we propose a further improved illumina-

tion model for rendering not only ideally smooth surfaces but also rough surfaces coated with various kinds of multilayer films. The ideally smooth surface is literally an ideal model. In the real world, every surface of objects has some amount of roughness, and reflected and/or transmitted light is dispersed on the real surface. Therefore, it is necessary to render rough surfaces for accurately visualizing various kinds of objects coated with multilayer films.

3. Optical phenomena due to multilayer films

In this section, we first explain optical phenomena due to multilayer film, and then derive a theoretical approach to compute a composite reflectance and transmittance[13] of a system of multilayer thin films.

3.1. Theoretical approach to a multilayer film system

Optical phenomena inside multilayer films is complex. Various kinds of physical phenomena, such as interference and absorption inside each layer, and reflection and transmission at each boundary, occur in the multilayer films, and they are complicatedly related with each other. Figure 2 shows the propagation of light inside the multilayer films. Light repeatedly reflects and transmits at the boundaries between films. After the multiple reflection and refraction, light reflects into the medium-A where the incident light comes, and transmits into a medium-B.

The reflected and refracted light with particular wave lengths are strengthened or weakened due to their phase differences. In addition to the interference, there is absorption of light inside semiconductive or metallic media. The absorption of light is explained by complex refractive indices which semiconductive or metallic media have.

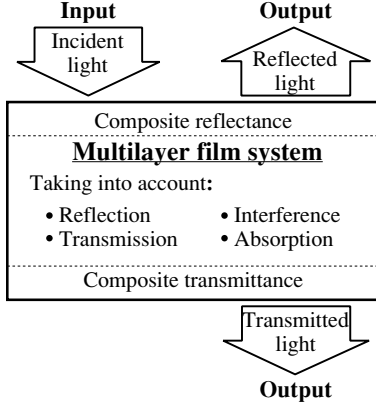To accurately render optical phenomena inside multilayer

Figure 3: *Theoretical approach of a multilayer film system.*

Figure 4: *Multilayer film system.*

films, it needs a huge computation cost to trace all rays inside the films taking into account the phenomena described above. To solve the problem, multilayer films are considered to be a single input-output system, and specific coefficients expressing the input-output relationship of the system calculated using coefficients of each layer (see Fig. 3). That is, a composite reflectance and transmittance of a multilayer film system are calculated from reflectivities and transmissivities of each boundary between films, taking into account interference and absorption of light inside each layer. This theoretical approach makes it possible to accurately visualize optical phenomena inside multilayer films. Next, we discuss a method for computing the composite reflectance and transmittance.

3.2. A method for calculating composite reflectance and transmittance[13]

We consider a $(N+2)$ layered film system (see Fig. 4), that is, there is a N layers of films between two media. Incident light from the medium-A is reflected back into the medium-A and transmitted into medium-B. Preconditions of a multilayer film systems in the proposed method are as follows.

1. Each boundary is parallel to *xy*-plane and smooth. For this precondition, light is reflected in only a mirror direction and transmitted in only a direction obeying Snell's law at each boundary.
2. Each layer is a homogeneous and isotropic medium, that is, a refractive index of each layer is constant.
3. Light comes in parallel to the *zx*-plane from medium-A. A refractive index of medium-A should be a real value, i.e., there is no absorption in the medium from which light comes.

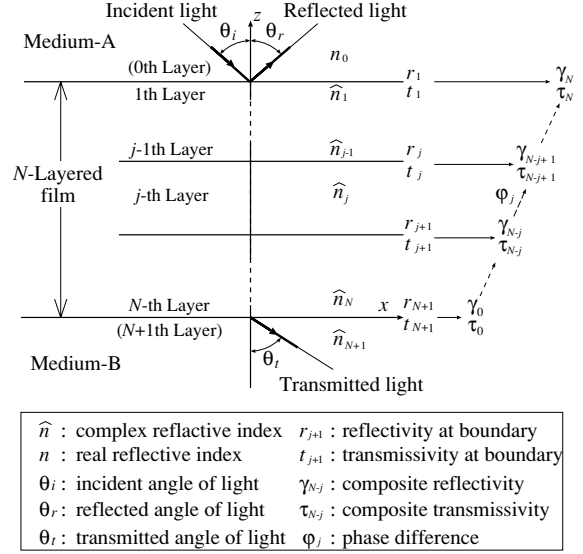According to these preconditions, a composite reflectance, γ_N, and transmittance, τ_N, of the $(N+2)$ layered film system

are calculated by an iterative method from the last layer to the first[13] (see Appendix A).

- Seed Eqs. (for $j = N+1$)

$$\gamma_0 = r_j = r_{N+1}, \tag{1}$$

$$\tau_0 = t_j = t_{N+1}. \tag{2}$$

- Recurrence Eqs. (for $j = N, \cdots, 1$)

$$\gamma_{N-j+1} = \frac{r_j + \gamma_{N-j}\, e^{2i\varphi_j}}{1 + r_j\, \gamma_{N-j}\, e^{2i\varphi_j}}, \tag{3}$$

$$\tau_{N-j+1} = \frac{t_j\, \tau_{N-j}\, e^{i\varphi_j}}{1 + r_j\, \gamma_{N-j}\, e^{2i\varphi_j}}, \tag{4}$$

where i denotes an imaginary number, r_j and t_j are the reflectivity and transmissivity at a boundary between $(j-1)$th and j-th layers, respectively, and these coefficients are obtained by Fresnel formulae. φ_j is the phase difference between boundaries of j-th layer. γ_{N-j} and τ_{N-j} are the composite reflectivity and transmissivity at a boundary between j-th and $(N+1)$th layers, respectively.

The reflectivity and transmissivity represent ratios of amplitudes of reflected and transmitted electromagnetic waves, respectively. On the other hand, the reflectance and transmittance represent ratios of energies of reflected and transmitted light, respectively, and they are obtained by square of an absolute value of the reflectivity and transmissivity. Finally, a composite reflectance, k_r, and transmittance, k_t, of the multilayer film system are calculated by averaging the energies of the parallel ($\parallel$) and perpendicular ($\perp$) components, because the contributions of these two components to the reflectance
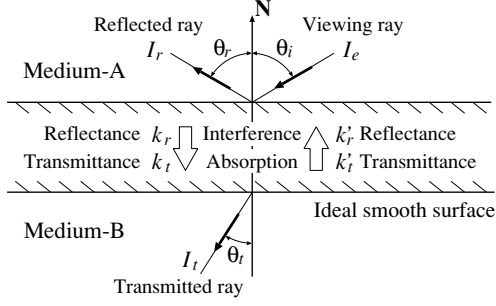
Figure 5: *Ideally smooth surface coated with multilayer films.*

(a) Global illumination component   (b) Local illumination component

Figure 6: *Rough surfaces coated with multilayer films.*

and transmittance are usually equal.

$$k_r = \frac{1}{2}\left(\left|\gamma_{\parallel,N}\right|^2 + \left|\gamma_{\perp,N}\right|^2\right), \tag{5}$$

$$k_t = \begin{cases} \dfrac{n_{N+1}\cos\theta_t}{n_0\cos\theta_i}\left[\dfrac{1}{2}\left(\left|\tau_{\parallel,N}\right|^2 + \left|\tau_{\perp,N}\right|^2\right)\right] & \\ \hfill (n_{N+1}:\text{real}) \\ 0 \hfill (n_{N+1}:\text{complex}), \end{cases} \tag{6}$$

where n_0 and n_{N+1} denote refractive indices of 0th and N-th layers, respectively, and the other arguments are illustrated in Fig. 4.

4. Illumination model

In this section, we discuss an illumination model to accurately render objects coated with multilayer films, taking into account multiple reflection, interference, and absorption of light. The illumination model consists of two kinds of models, depending on reflection properties of object surfaces on which multilayer films are coated: Ideally smooth and locally smooth rough surfaces (LSRS type)[15].

4.1. Ideally smooth surfaces

In this type of surfaces, the proposed method described in Sec. 3.2 can be directly used to calculate a composite reflectance and transmittance, because all boundary surfaces consisting of multilayer film system are smooth. Therefore, the equation of the illumination model is expressed as follows (see Fig. 5).

$$I_e(\lambda) = k_r(\theta_i,\lambda)I_r(\lambda) + k_t(\theta_i,\lambda)I_t(\lambda), \tag{7}$$

where I_e, I_r, and I_t indicate intensities of an viewing, reflected, and transmitted rays, respectively. θ_i is an incident angle of the viewing ray, and λ is wave length of light. k_r and k_t are a reflectance and transmittance of the multilayer film system obtained by the composite reflectance and transmittance calculation described in Eqs. 5 and 6. Note that we can use a forward transmittance, $k_t(\theta_i,\lambda)$, in Eq. 7, as the
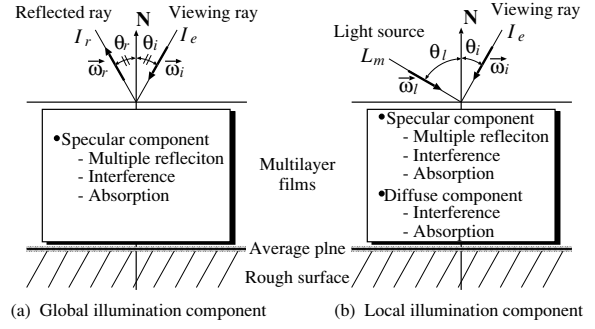
forward transmittance is equivalent to the backward transmittance, $k_t'(\theta_t,\lambda)$, because of the energy conservation law.

4.2. Rough surfaces

Rough surfaces consist of micro facets, and these surfaces are gentle roughness slopes. Multilayer films coated on the surface have still smooth boundaries between films because we assume that the bump of the rough surface is quite small compared with the extent of the surface. Thickness of a layer adjoined by the rough surfaces is approximated by averaging height of the micro facets. The equation of the illumination model is expressed as follows.

$$I_e(\lambda) = k_r(\theta_i,\lambda)I_r(\lambda) + \sum_{m=1}^{M} k_d(\vec{\omega}_l,\vec{\omega}_i,\lambda)\cos\theta_l L_m(\lambda), \tag{8}$$

where k_d is a diffuse reflection coefficient including directional and uniform diffuse components, $\vec{\omega}$ represents a direction of (θ,ϕ), and L_m denotes an intensity of each light source ($m = 1,\cdots,M$; M is the number of light sources). The first and second terms express global and local illumination components, respectively (see Fig. 6).

For global illumination components, their intensities are calculated by tracing a reflected ray recursively and multiplying specular reflectances, k_r, at each intersection point. The composite specular reflectivity, $\gamma_{s,N}$, of a rough surface coated with multilayer films is calculated by the following seed and recurrence equations.

$$\gamma_{s,0} = \eta(\vec{\omega}_{i,N},\vec{\omega}_{i,N},\lambda), \tag{9}$$

$$\gamma_{s,N-j+1} = \frac{r_j(\theta_{i,j-1},\lambda) + \gamma_{N-j}(\theta_{i,j},\lambda)\,e^{2i\varphi_j(\theta_{i,j},\lambda)}}{1 + r_j(\theta_{i,j-1},\lambda)\,\gamma_{N-j}(\theta_{i,j},\lambda)\,e^{2i\varphi_j(\theta_{i,j},\lambda)}} \tag{10}$$
$$(\text{for } j = N,\cdots,1),$$

where η expresses a ratio of amplitude of electromagnetic waves taking into account roughness of object surfaces, and depends on both directions of an incident and reflected light.
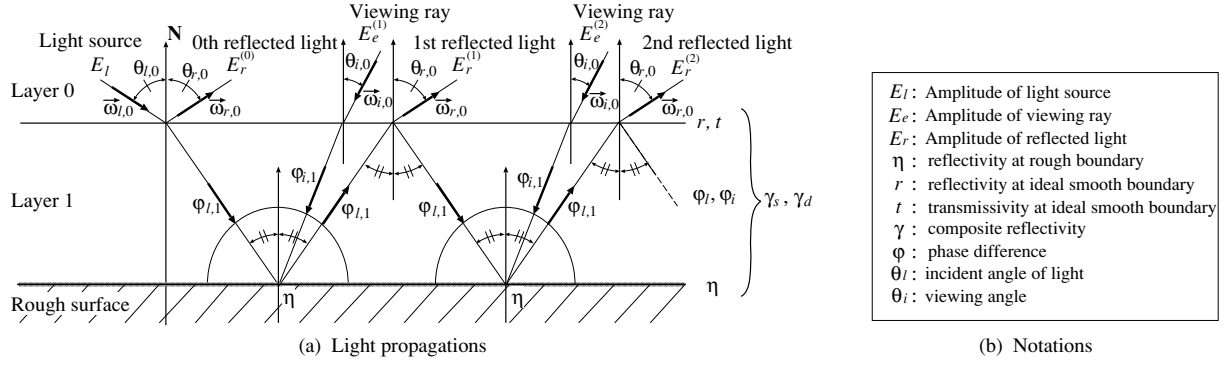
Figure 7: *Specular and diffuse component of light.*

Finally, the specular reflectance, k_r, is obtained from a composite reflectivity, $\gamma_{s,N}$, using Eq. 5. For the specular reflectance of rough surfaces, multiple reflections, interference, and absorption of light inside all layers are taken into account.

To calculate the diffuse reflectance, k_d, we assume the following model. As shown in Fig. 7, a locally smooth rough surface is coat with a single layer, and light is reflected toward a viewpoint. A specular component of light inside the layer is reflected repeatedly on the both boundaries, that is, multiple reflections of a specular component should be taken into account. On the other hand, a diffuse component is relatively small, compared to the specular component, and a primary reflection of the diffuse component is only taken into account. From the above discussion, amplitudes of the reflected light into the viewing direction as follows.

$$E_e = \sum_{m=1}^{\infty} \Gamma \Lambda^{m-1} E_l, \qquad (11)$$

where,

$$\Lambda = -r(\theta_{l,0},\lambda)\eta(\vec{\omega}_{l,1},\vec{\omega}_{l,1},\lambda)e^{2i\varphi_{l,1}(\theta_{l,1},\lambda)}, \qquad (12)$$

$$\Gamma = \frac{\widehat{n}_1 s_{z,1}}{\widehat{n}_0 s_{z,0}} t(\theta_{i,0},\lambda)t(\theta_{l,0},\lambda)\eta(\vec{\omega}_{l,1},\vec{\omega}_{i,1},\lambda)\Phi_{l,1}, \qquad (13)$$

$$\Phi_{l,1} = e^{i[\varphi_{l,1}(\theta_{l,1},\lambda)+\varphi_{i,1}(\theta_{i,1},\lambda)]}, \qquad (14)$$

where m denotes the number of multiple reflection, $\widehat{n}$ is a refractive index, and s_z is a z-component of the unit vector indicating a direction of the light propagation. From these equations, the recurrence equations to calculate composite reflectance are obtained by the similar way to that of Eqs. 3 (see Appendix A). For local illumination, a composite diffuse reflectivity, $\gamma_{d,N}$, is calculated by the following seed and recurrence equations.

$$\gamma_{d,0} = \eta(\vec{\omega}_{l,N},\vec{\omega}_{i,N},\lambda), \qquad (15)$$

$$\gamma_{d,N-j+1} = \frac{\Gamma_j}{1+r_j(\theta_{l,j-1},\lambda)\gamma_{s,N-j}(\theta_{l,j},\lambda)e^{2i\varphi_{l,j}(\theta_{l,j},\lambda)}} \qquad (16)$$

$$(\text{for } j = N, \cdots, 1),$$

where

$$\Gamma_j = \frac{\widehat{n}_j s_{z,j}}{\widehat{n}_{j-1} s_{z,j-1}} t_j(\theta_{i,j-1},\lambda)t_j(\theta_{l,j-1},\lambda) \cdot$$
$$\gamma_{d,N-j}(\vec{\omega}_{l,j},\vec{\omega}_{i,j},\lambda)e^{i[\varphi_{l,j}(\theta_{l,j-1},\lambda)+\varphi_{i,j}(\theta_{i,j-1},\lambda)]}, \qquad (17)$$

where γ_s is a composite specular reflectivity, and is calculated by using Eqs. 9 and 10. Consequently, a diffuse reflectance, k_d, is obtained by the composite reflectivity, $\gamma_{d,N}$, using Eq. 5.

5. Implementation

We implemented the proposed method into a Multilayer Film Raytracer (MFRT)[13]. The MFRT has been developed to accurately visualize optical phenomena due to multilayer films.

Composite reflectances and transmittances of multilayer film systems are pre-calculated by using the proposed method described in Sec. 4 for each sampled incident angle and wave length of light, and stored into tables before the raytracing process. In the rendering process, if a ray intersects with an object coated with films, a reflectance and transmittance at the intersection are linearly interpolated from the pre-calculated tables.

6. Examples

Figure 8 and 9 shows examples rendered by the proposed method. We employed a He-Torrance model[16] to define reflection properties of the rough surfaces, and the spectral distribution of light sources is set to a fluorescent lamp (N)[17].

(a) Silicon spheres ($\sigma_0 = 0$ [nm]) (b) Silicon spheres ($\sigma_0 = 25$ [nm]) (c) Silicon spheres ($\sigma_0 = 50$ [nm])

(d) Aluminum spheres ($\sigma_0 = 0$ [nm]) (e) Aluminum spheres ($\sigma_0 = 25$ [nm]) (f) Aluminum spheres ($\sigma_0 = 50$ [nm])

(g) Aluminum spheres ($\sigma_0 = 0$ [nm]) (h) Aluminum spheres ($\sigma_0 = 25$ [nm]) (i) Aluminum spheres ($\sigma_0 = 50$ [nm])
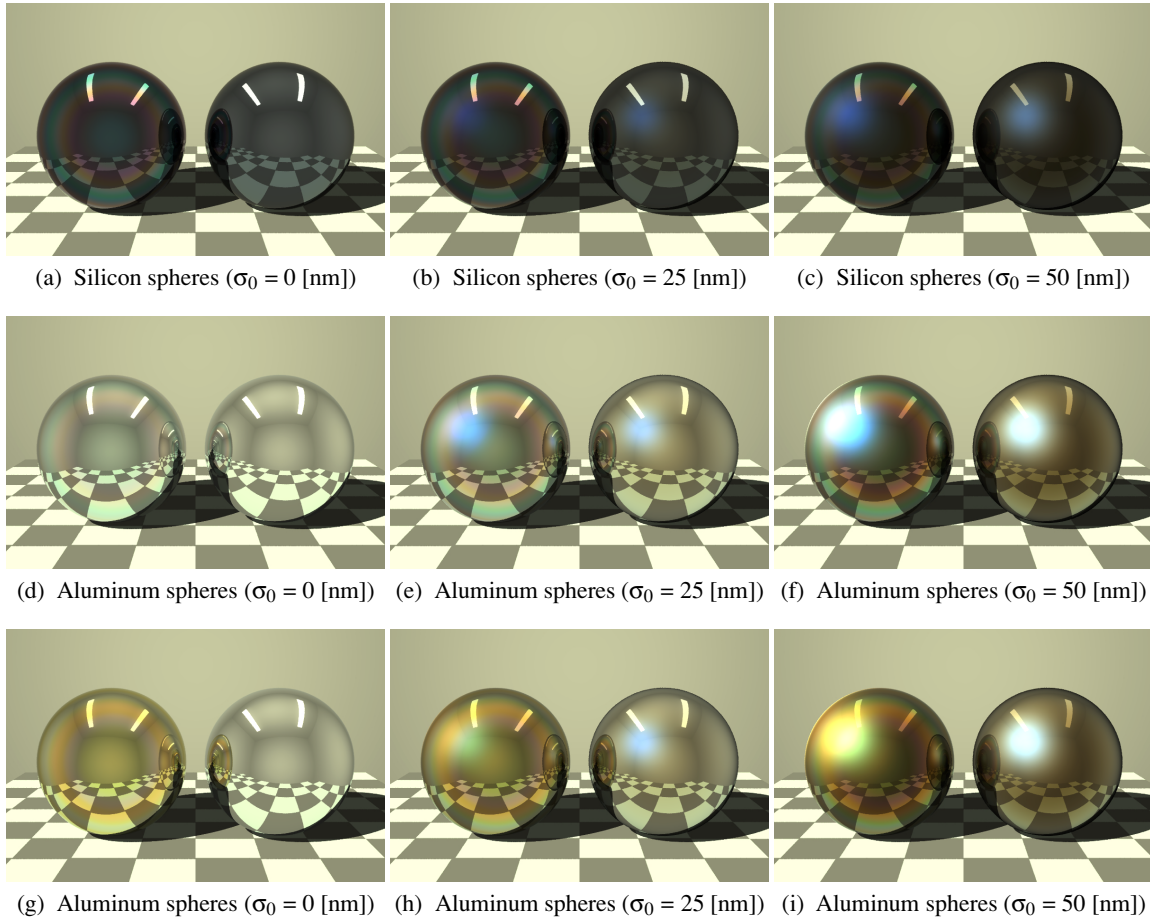
Figure 8: *Rough surfaces and ideally smooth surfaces coated with multilayer films.*

Spheres shown in Figs. 8(a)–(c) are made of silicon, and spheres shown in Figs. 8(d)–(i) are made of aluminum. The left-hand sphere is coated with multilayer films, and the right-hand one is not. Parameters of the rough surfaces (rms roughness[16], σ_0, and autocorrelation length[16], τ) are set to $\sigma_0 = 0$ [nm] in Figs. 8(a), (d), and (g); $\sigma_0 = 25$ [nm] in Figs. 8(b), (e), and (h); $\sigma_0 = 50$ [nm] in Figs. 8(c), (f), and (i); and $\tau = 300$ [nm] for all figures. Note that surfaces of spheres are ideally smooth when $\sigma_0 = 0$ [nm]. The left-hand sphere in Figs. 8(a)–(f) is coated with three-layer films consisting of dielectric, silver, and dielectric layers, and the left-hand sphere in Figs. 8(h)–(i) is also coated with three-layer films consisting of dielectric, gold, and dielectric layers. The refractive index and the thickness of the dielectric layer are set to 1.4 and 1000 [nm], respectively. The thicknesses of the silver and gold layers are set to 5 [nm].

Iridescent colors caused by interference and absorption of light inside the multilayer films can be observed on the surfaces of the left-hand spheres. Furthermore, the iridescent colors on the rough surfaces in Figs. 8(e), (f), (h), and (i) ap-

pear more clearly than those on the ideally smooth surfaces in Figs. 8(d) and (g). This is because reflected light from the rough surfaces is weaker than that of the ideally smooth surfaces due to the roughness, and the iridescent colors are emphasized.

In Fig. 9, a teapot, a cylinder, and a sphere are made of aluminum, silicon, and copper, respectively. The surfaces of objects in Fig. 9(a) are ideally smooth surfaces, while those in Fig. 9(b) are rough surfaces. Table 1 shows a specification of multilayer films and parameters of roughness used for each object in Fig. 9. The iridescent colors on the rough surfaces appear more clearly than those on the ideally smooth surfaces.

The size of the rendered images in Fig. 9 is 800×533 pixels, and it took 100 minutes to render each image with 2×2 super sampling per a pixel on a Pentium II CPU (450MHz).

Figures 8 and 9 demonstrate the usefulness of the proposed method for visualizing the optical phenomena caused
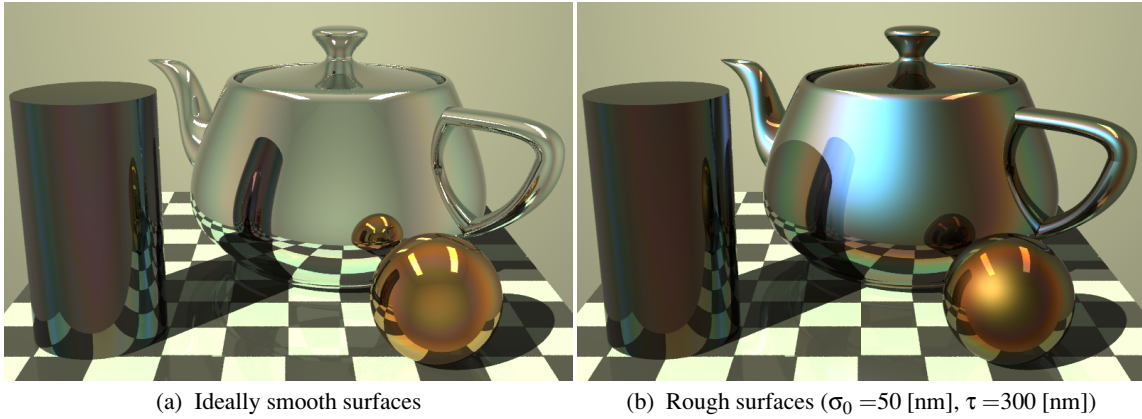
(a) Ideally smooth surfaces   (b) Rough surfaces (σ_0 =50 [nm], τ =300 [nm])

Figure 9: *Comparison of ideally smooth surfaces and rough surfaces coated with multilayer films.*

Table 1: *The multilayer film systems used in Fig. 9.*

	The system of multilayer films (medium-A, 1st layer, 2nd layer, $\cdots$, medium-B)
Teapot	air, dielectric A (1000 [nm]), silver (5 [nm]), dielectric A (1000 [nm]), aluminum
Cylinder	air, dielectric B(1000 [nm]), dielectric A(1000 [nm]), dielectric B(1000 [nm]), dielectric A(1000 [nm]), silicon
Sphere	air, dielectric A (1000 [nm]), gold (5 [nm]), dielectric A (1000 [nm]), copper

dielectric A: n =1.4, dielectric B: n =2.0, (n: refractive index)

by multilayer film systems, taking into account the roughness of surfaces coated with the films.

7. Conclusions

We have proposed an accurate illumination model for rendering objects coated with multilayer films. The proposed method makes it possible to visualize accurate reflectance and transmittance properties of objects coated with multilayer films. The illumination model can handle both smooth surface and locally smooth rough surfaces, and visualize optical effects caused by multilayer films, taking into account multiple reflection and refraction, interference and absorption of light inside this films.

One of the future studies is developing a method for considering the geometry of rough surfaces, that is, a rough surface is modeled as a bump surface instead of a smooth averaging surface with roughness. Developing the method, both interference due to multilayer films and diffraction due to bump surfaces can be rendered at the same time.

References

1. H. P. Moravec. 3d graphics and the wave theory. *Proc. SIGGRAPH 81. In Computer Graphics*, 15(3):289–296, 1981. 1

2. E. Nakamae, K. Kaneda, T. Okamoto, and T. Nishita. A lighting model aiming at drive simulators. *Proc. SIGGRAPH 90. In Computer Graphics*, 24(4):395–404, 1990. 1

3. I. Icart and D. Arques. An illumination model for a system of isotropic substrate- isotropic thin film with identical rough boundaries. *Proc. the 10th Eurographics Workshop on Rendering*, pages 261–272, 1999. 1, 2

4. N. Suzuki, S. Yokoi, and J. Toriwaki. Study on color computation in computer graphics and it's application to rendering color caused by light interference. *IEICE Technical Report of Japan*, 88(450):41–48, 1993. (in Japanese). 1

5. B. E. Smits and G. W. Meyer. Newton's colors: Simulating interference phenomena in realistic image synthesis. *Proc. Eurographics Workshop on Photosimulation, Realism and Physics in Computer Graphics*, pages 185–194, 1990. 1

6. M. L. Dias. Ray tracing interference color. *IEEE Computer Graphics and Applications*, 11(2):54–60, 1991. 1

7. J. Li and Q. Peng. A new illumination model for scenes

containing thin film interference. *Chinese Journal of Electronics*, 5(1):18–24, 1996. 1

8. M. L. Dias. Ray tracing interference color: Visualizing newton's rings. *IEEE Computer Graphics and Applications*, 14(3):17–20, 1994. 2

9. J. S. Gondek, G. W. Meyer, and J. G. Newman. Wavelength dependent reflectance functions. *Proc. SIGGRAPH 94*, pages 213–220, 1994. 2

10. P. Hanrahan and K. Wolfgang. Reflection from layerd surfaces due to subsurfaces scattering. *Proc. SIGGRAPH 93*, pages 165–174, 1993. 2

11. N. Nagata, T. Dobashi, Y. Manabe, T. Usami, and S. Inokuchi. Modeling and visualization for a pearl-quality evaluation simulator. *IEEE Trans. Visualization and Computer Graphics*, 3(4):307–315, 1997. 2

12. J. Dorsey and P. Hanrahan. Modeling and rendering of metallic paints. *Proc. SIGGRAPH 96*, pages 387–396, 1996. 2

13. H. Hirayama, Y. Monden, K. Kaneda, and H. Yamashita. Scientific visualization of wave scattering phenomena of transparent optical systems. *The Journal of Institute of Image Electronics Engineers of Japan*, 27(4):306–317, 1998. (in Japanese). 2, 3, 5

14. H. Hirayama, K. Kaneda, H. Yamashita, Y. Monden, and Y. Yamaji. Visualization of optical phenomena caused by multilayer films with complex refractive indices. *Proc. Pacific Graphics '99*, pages 128–137, 1999. 2

15. I. Ohlidal and K. Navratil. Scattering of light from multilayer systems with rough boundaries. *Progress in Optics*, 34, 1995. 4

16. X. D. He, K. E. Torrance, F. X. Sillion, and D. P. Greenberg. A comprehensive physical model for light reflection. *Proc. SIGGRAPH 91. In Computer Graphics*, 25(4):175–186, 1991. 5, 6

17. Ed. The Illuminating Engineering Institute of Japan. *Lighting Handbook*. Ohmsha, 1987. (in Japanese). 5

Appendix A: Recurrence equations of composite reflectivity and transmissivity

Let's consider a three-layer film system (see Fig. 10), where light comes form layer, L_0, and is transmitted to layer, L_2, with multiple reflection inside layer, L_1. Assuming that the forward reflectivity and transmissivity at boundary, B_1, are r_1 and t_1, respectively, and the backward reflectivity and transmissivity, i.e., those which light travels from layer, L_1 to layer, L_0, are r_1' and t_1', respectively, the composite reflectivity, γ, and transmissivity, τ, of the three-layer system are
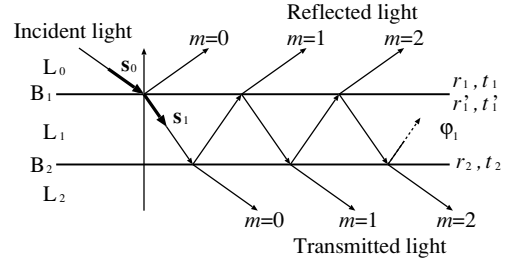

Figure 10: *The three-layer film system.*

expressed as follows:

$$\gamma = r_1 + \sum_{m=1}^{\infty} t_1 r_2 \left(r_1' r_2 \right)^{m-1} t_1' e^{2i\varphi_1 m}, \qquad (18)$$

$$\tau = \sum_{m=0}^{\infty} t_1 \left(r_2 r_1' \right)^m t_2 e^{i\varphi_1(2m+1)}, \qquad (19)$$

where φ_1 is the phase difference between the boundaries of layer, L_1. Note that these equations are infinite geometric series, because of the multiple reflection of light between the boundaries of layer, L_1.

Using the relationships between the forward and backward reflectivities/transmissivities,

$$\gamma = \lim_{m \to \infty} \frac{r_1 + \left(r_1^2 + \frac{\widehat{n}_1 s_{z,1}}{\widehat{n}_0 s_{z,0}} t_1^2 \right) r_2 e^{2i\varphi_1}}{1 + r_1 r_2 e^{2i\varphi_1}}$$
$$- \frac{r_2 \frac{\widehat{n}_1 s_{z,1}}{\widehat{n}_0 s_{z,0}} t_1^2 e^{2i\varphi_1} \left(-r_1 r_2 e^{2i\varphi_1} \right)^m}{1 + r_1 r_2 e^{2i\varphi_1}}, \qquad (20)$$

$$\tau = \lim_{m \to \infty} \frac{t_1 t_2 e^{i\varphi_1} - t_1 t_2 e^{i\varphi_1} \left(-r_1 r_2 e^{2i\varphi_1} \right)^m}{1 + r_1 r_2 e^{2i\varphi_1}}. \qquad (21)$$

From Fresnel formulae, the following equation is derived.

$$r^2 + \frac{\widehat{n}_1 s_{z,1}}{\widehat{n}_0 s_{z,0}} t^2 = 1. \qquad (22)$$

Equations 20 and 21 converge as the absolute value of the common ratio of the geometric series satisfies that $\left| r_1 r_2 e^{2i\varphi_1} \right| < 1$. Finally, the composite reflectivity and transmissivity of the three-layer film system are derived as follows:

$$\gamma = \frac{r_1 + r_2 e^{2i\varphi_1}}{1 + r_1 r_2 e^{2i\varphi_1}}, \qquad \tau = \frac{t_1 t_2 e^{i\varphi_1}}{1 + r_1 r_2 e^{2i\varphi_1}}. \qquad (23)$$

Repeating this process in order of layers from the transmitted light to the incident light, i.e., the inverse direction of transmission of light, the recurrence equations (Eqs. 3 and 4) are obtained.

$$\gamma_{N-j+1} = \frac{r_j + \gamma_{N-j} e^{2i\varphi_j}}{1 + r_j \gamma_{N-j} e^{2i\varphi_j}}, \quad \tau_{N-j+1} = \frac{t_j \tau_{N-j} e^{i\varphi_j}}{1 + r_j \gamma_{N-j} e^{2i\varphi_j}}. \qquad (24)$$